



## Analysis of the Thermoluminescent Glow Curve of Alumina Matrices Obtained Under Different Sintering and Cerium Doped Conditions

---

Jorge Rojas, Rafael Cogollo and Omar Gutiérrez

EasyChair preprints are intended for rapid dissemination of research results and are integrated with the rest of EasyChair.

August 26, 2021

# Analysis of the thermoluminescent glow curve of alumina matrices obtained under different sintering and cerium doped conditions

J Rojas<sup>1</sup>, R Cogollo<sup>1,3</sup>, O Gutiérrez<sup>2</sup>

<sup>1</sup> Grupo de Materiales y Física Aplicada, Facultad de Ciencias Básicas, Universidad de Córdoba, Carrera 6A #77-305, Montería, Colombia

<sup>2</sup> Grupo Alquimia, Facultad Ciencias Exactas y Aplicadas, Instituto Tecnológico Metropolitano, Calle 73 No 76A-354 Vía al Volador, Medellín, Colombia

E-mail: rafaelcogollo@gmail.com

**Abstract.** This work presents the deconvolution of thermoluminescent (TL) glow curves, by using logistic asymmetric functions, of sintered pure alumina matrices under two different conditions: 1000 °C/3h (NALO) and 1000 °C/6h (ALO), and also, of cerium-doped matrix with 0.1 wt.% sintered at 1000 °C/3h (NALOCe0.1). Sintering treatments induced a remarkable change in the TL kinetics and consequently in the glow curve shape, in terms of the number of traps and initially trapped charge carriers. Structural analysis revealed  $\alpha$ -alumina phase in NALO and ALO matrices, and its distortion for NALOCe0.1, achieving a generation of new electronic traps energetically more stable for doped matrix. This result offers a possible solution in order to reduce the notable fading for TL characteristic peak in alumina matrix, expanding its field of applications.

## 1. Introduction

The main practical application of thermoluminescence (TL) is radiation dosimetry, an activity in which there has been a great development among the international scientific community since the initial work of Daniels et al. In the search for new useful materials such as TL dosimeters,  $\alpha$ -Al<sub>2</sub>O<sub>3</sub> has been reported in the literature for use in clinical, personal and environmental monitoring of ionizing radiation [2-7]. The  $\alpha$ -Al<sub>2</sub>O<sub>3</sub> has a high sensitivity TL that allows it to have a low dose limit, property that is sensitive with the concentrations of the impurities, the conditions of growth of the crystal and thermal treatment of the grown crystals [2,8], reason why it is necessary to find new variations of the material that conserve its sensitivity and reduce its weaknesses like the decay of the signal with time [7]. One of these typical variations is doping with carbon [9] and with cerium [10], the latter being found to act as an activator. However, the influence of cerium on the TL kinetics of the glow curve of alumina matrices has not yet been reported in the literature. In addition, the glow curve is often made up of more than one signal, so that the theories developed for first-, second- and general order kinetics in a single peak TL [11] are insufficient to analyze these complex TL curves [12,13]. Among the methods that allow the separation of these curves into their individual components, the deconvolution with logistic asymmetric functions

---

<sup>3</sup> To whom any correspondence should be addressed.

(LAF) proposed by Pagonis and Kitis [14] has gained a special interest because it allows the correlation of the LAF parameters with the kinetic parameters of the thermoluminescent response.

Considering the potential technological applications of cerium-doped alumina matrices for the field of radiation dosimetry, and the importance of TL curves for obtaining information on the kinetic parameters and TL behaviour of the material, this work addresses the effect of calcination conditions and cerium doping on these alumina matrices.

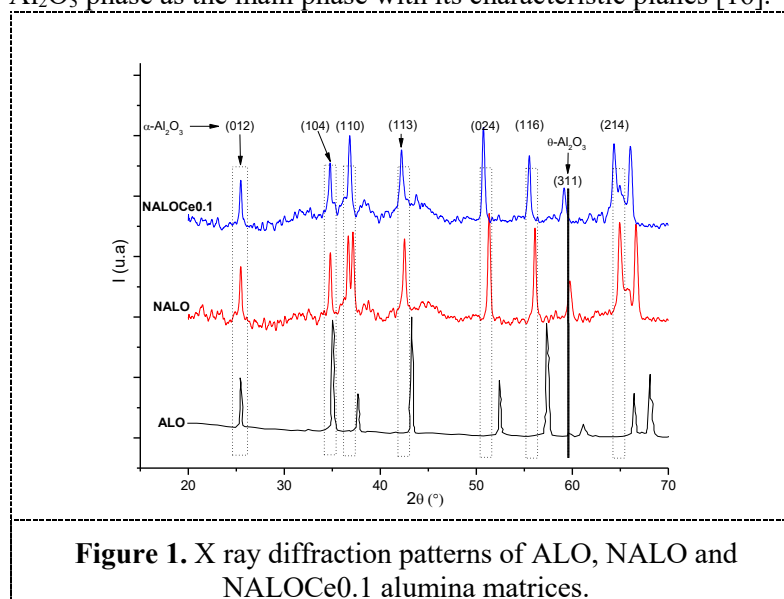
## 2. Material and Method

Boehmite alumina powder (purity 99.995%, W. R. Grace & Co-Conn) was used to prepare sintered pills of 5 mm diameter and 1 mm thickness. The samples were initially compacted at two tons of pressure and subsequently sintered at 1000 °C in air in a D8 Ground furnace using a heating rate of 1 °C/min. The first group of matrices called NALO was sintered for 1 hour, then the samples were ground and compacted again to be sintered at 1000 °C for another 1 hour, then the samples were ground and compacted again at the same pressure and sintered at the same temperature for another hour. The second group called ALO was sintered at the same temperature for 3 hours, then the samples were ground and compacted to be sintered again at 1000 °C for another 3 hours. A third group of alumina matrices doped with 0.1 wt% of cerium (NALOCe0.1) was prepared using the wet impregnation method, using cerium nitrate hexahydrate (purity 98.5%, MERCK). The same sintering conditions of the NALO matrices were applied to the doped samples. The sintered pills were analyzed by X-ray diffraction (Panalytical Empyrean Serie II – Alpha1, model 2012) with a Cu ceramics source with a  $K_{\alpha 1}$   $\lambda=1.5406$  Å radiation. All samples were irradiated in air at room temperature at a dose of 10 Gy using a linear accelerator (LINAC) using three replicates per sample. The samples were read at a TLD 4500, at a heating rate of 5 K/s between 324 K and 672 K according to the procedure described in [7]. The glow curves were analyzed by using deconvolution with LAF and Rasheedy's methodology. The kinetic parameters: kinetic order parameter (b), activation energy (E), the pre-exponential factor ( $S''$ ) and the initial concentration of trapped electrons ( $n_0$ ); were found as described in [15].

## 3. Results and Discussion

### 3.1. Structural Analysis

Figure 1 shows the diffraction patterns of the ALO, NALO and NALOCe0.1 matrices indicating the presence of the  $\alpha$ - $Al_2O_3$  phase as the main phase with its characteristic planes [16].

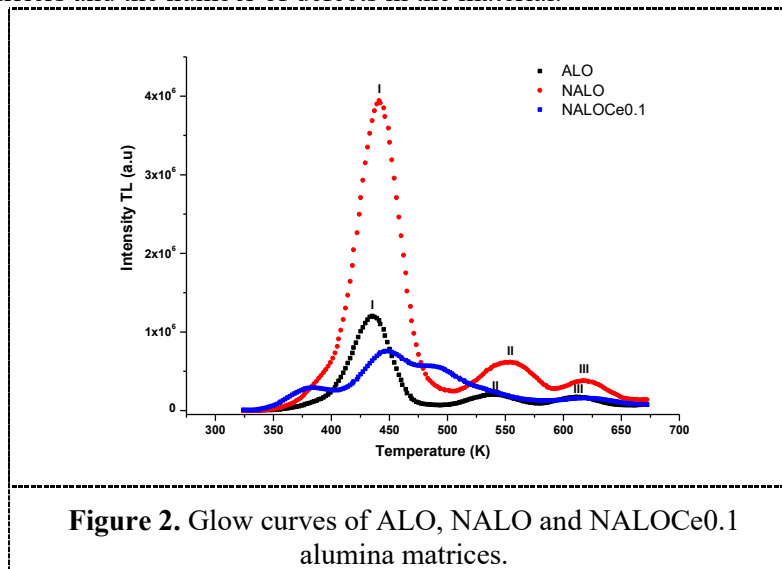


The pure alumina matrix also shows the presence of the phase  $\theta$ - $Al_2O_3$  with its characteristic reflection in the plane (311). Furthermore, in the cerium-doped matrices a shift towards lower angles can be

observed for the planes (104), (113), (024), (116), (311) and (214); indicating an increase in the interplanar distance characteristic of these planes.

### 3.2. Thermoluminescent behavior of sintered alumina matrices

Figure 2 shows the glow curve of ALO sample. The curve shows three peaks located at 436 (peak I), 538 (peak II) and 611 K (peak III) respectively. The NALO sample showed a similar glow curve, but with a slight shift in the position of the main peak with temperature values of 443 (peak I), 554 (peak II) and 623 K (peak III) respectively. The main peak (peak I) according to Osorio et al. [7] is optimal for radiation dosimetry. There is also a difference in the TL intensities of the ALO and NALO samples, with higher intensities observed in the peaks of the NALO sample, which is related to the number of trapped charge carriers and the number of defects in the material.



The lower intensity in the ALO sample curve is due to a lower concentration of defects or traps in the material, implying a lower concentration of electrons in traps and voids in recombination centers. This is due to the fact that the ALO samples, when receiving a longer heat treatment (1000 °C/6 h) with respect to the NALO sample (1000 °C/3 h), have fewer imperfections and metastable energy states in the material structure, releasing a lower number of trapped charge carriers [7].

For the NALOCe0.1 sample, a significant decrease in TL intensity is observed compared to the NALO sample, indicating a reduction in sensitivity of the material due to the introduction of cerium impurities. However, it should be noted, that the main peak of the glow curve remains almost in the same position (~444 K). The NALOCe0.1 sample shows a complex TL curve consisting of more than three experimental signals, showing that doping can stimulate the appearance of new types of traps in the crystal lattice by modifying the glow curve of the NALO samples. In addition, the width of the diffraction peaks (figure 1) indicates the presence of amorphous phases caused by cerium, which can introduce defects during the crystal growth process, explaining the redistribution of the number and type of energy traps with respect to the NALO matrix [7]. In addition, a shift of the trap of greater energy depth towards higher values of temperature with respect to the NALO matrix is observed. It is also clear a remarkable growth of peak 1 of the NALO matrix located around 380 K with a shift towards lower temperature values, which could lead to a premature emptying of the trap.

### 3.3. Deconvolution of the glow curves of ALO, NALO and NALOCe0.1 samples

In figure 3a the deconvolution for the ALO sample shows that the three TL signals (I, II, III) in figure 2 are due only to the presence of three different types of energy traps. While figure 3b shows that for the NALO matrix these three main signals (figure 2) are due to the presence of four energy traps. This

effect is a clear consequence of the heat treatment used during sintering of the samples. The NALOCe0.1 sample has six energy traps.

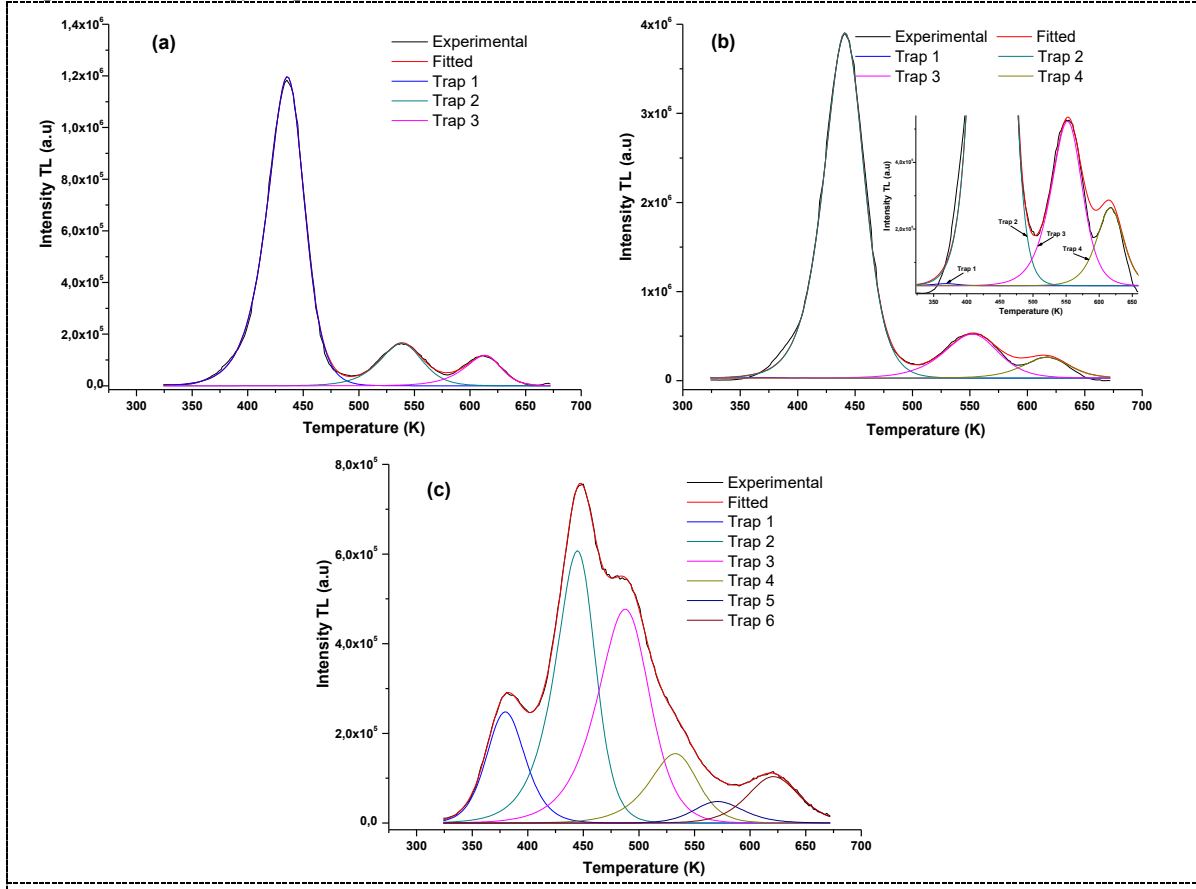


**Figure 3.** Deconvolution of the glow curves of ALO, NALO and NALOCe0.1 alumina matrices.

From the logistic parameters of the LAF obtained with the deconvolution in the ALO, NALO and NALOCe0.1 matrices, the kinetic parameters of the glow curves were calculated and compiled in table 1.

**Table 1:** Deconvolution kinetic parameters of samples of ALO, NALO and NALOCe0.1.

Kinetic Parameters	ALO			NALO				NALOCe0.1					
	Trap 1	Trap 2	Trap 3	Trap 1	Trap 2	Trap 3	Trap 4	Trap 1	Trap 2	Trap 3	Trap 4	Trap 5	Trap 6
$T_m$ (K)	435	538	613	387	441	552	617	379	444	488	532	571	620
$I_m$ (a.u.)	1.20E+06	1.64E+05	1.17E+05	1.25E+05	3.87E+06	4.93E+05	2.34E+05	2.48E+05	6.07E+05	4.77E+05	1.55E+05	4.80E+04	1.03E+05
$b$	1.25	1.43	1.62	1.20	1.41	1.42	1.5	1.69	1.40	1.78	1.64	1.87	1.66
$E$ (eV)	1.14	1.49	1.83	1.02	1.11	1.33	1.58	0.88	1.29	1.40	1.68	1.71	1.86
$S''$ (s <sup>-1</sup> )	1.97E+12	7.06E+12	6.92E+13	2.85E+12	4.17E+11	7.79E+10	2.57E+11	5.27E+10	5.97E+13	2.16E+13	6.99E+14	6.97E+13	6.97E+13
$n_0$ (cm <sup>-3</sup> )	9.77E+06	1.71E+06	1.39E+06	8.85E+05	3.64E+07	7.03E+06	4.42E+06	2.34E+06	4.88E+06	4.93E+06	1.51E+06	6.00E+05	1.00E+06
FOM (%)	1.16			0.95				0.40					

A general order kinetics for all samples is shown in table 1. The kinetic order  $b$ , indicates that for the ALO matrices the recombination prevails over the re-trapping as a mechanism of deactivation of the energy traps for the main peak ( $b=1.25$ ), while for the NALO matrix the kinetic order ( $b=1.41$ ) suggests a mixed deactivation mechanism. This shows that the heat treatment modifies the kinetics of the material and not only the positions and shapes of the peaks in the glow curve. With regard to the peaks of higher

temperature (II and III of the glow curve) in both cases mixed deactivation processes are observed with a slight tendency to re-trapping in the ALO matrix especially in the trap with the highest energy depth. It should be noted that the main peak presents a lower intensity for the ALO sample, corresponding in the table to the number of charge carriers initially trapped.

The previous result, as mentioned above, is due to the fact that the ALO sample was sintered for much longer (3 more hours), possibly leaving fewer defects in the crystalline structure of the material, and therefore a lower concentration of available traps. This change in the thermal process may also be responsible for the appearance of the new type of traps in the NALO sample. According to Osorio et al. [7], this effect is in agreement with the results obtained in the structural analysis carried out by X-ray diffraction, where it is evident that the samples corresponding to the NALO sample exhibit different crystallographic phases and even the presence of amorphous phases, which leads to an increase in the number of defects in the material. It is also evident that the E values increase as the peaks are displaced at higher temperatures, since the depth of the traps is greater and a greater amount of energy is required to release the trapped charge carriers. The minimum (1.14 eV) and maximum (1.83 eV) E values in the ALO matrix were higher than their corresponding values in the NALO matrix (1.02 - 1.58 eV). This result indicates that the heat treatment applied in the ALO matrix in addition to reducing the number of traps gives them greater thermal stability. The pre-exponential factors present values within the theoretical estimate ( $10^{10}$  -  $10^{13}$  s<sup>-1</sup>). Additionally, for  $n_0$  there is a difference of an order of magnitude in the main peak when varying from  $10^7$  in the NALO matrix to  $10^6$  in the ALO matrix.

The six traps present in the glow curve of the NALOCe0.1 matrix show that cerium doping stimulates the appearance of new types of traps (peaks 3 and 5), with respect to the NALO matrix, since in principle traps 1, 2, 4 and 6 must come from the same type of traps as those exhibited by the NALO matrix, a reasonable assumption taking into account the proximity of the temperatures of the maximum intensity of each signal, as well as the value of the maximum intensities which are of the order of  $10^5$ .

The main peak exhibits a mixed deactivation mechanism ( $b=1.40$ ) the same as NALO, but the other peaks of the glow curve show a clear tendency towards re-trapping processes as a deactivation mechanism reaching values of the kinetic order of up to 1.78 (peak 3) and 1.87 (peak 5) unreachable in pure samples. In addition, the traps with higher temperatures (Peak 5 and Peak 6) had a remarkable shift towards greater energy depths while the first signal (Peak 1) did the opposite, i.e. towards lower temperature values. All these changes show how the sintering conditions and the introduction of cerium impurities have changed the positions, shapes and sizes of the peaks in the glow curve [3].

The above results show that  $n_0$  decreased with the introduction of cerium impurities into the pure matrix, this trend being more evident at the main peak TL, where  $n_0$  decreased by one order of magnitude. This remarkable decrease in the main peak should be taken into account for practical applications in TL dosimetry, since this phenomenon indicates a significant decrease in the sensitivity of the material. Regarding the pre-exponential factor, values between  $10^{10}$  and  $10^{14}$  s<sup>-1</sup> according to the kinetic theory were found for all samples. However, it should be kept in mind that high values of the pre-exponential factor ( $10^{14}$  s<sup>-1</sup>) influence the stability of the energy traps causing a premature thermal weakening of the signal.

The FOM (figure of merit) values obtained (less than 5.0 %) in all cases indicates that the proposed number of traps fits the experimental glow curves quite well [17].

#### 4. Conclusion

The heat treatments applied modified the thermoluminescent kinetics of the alumina matrices, in terms of the number of traps and the initial amount of  $n_0$  trapped load carriers.

The kinetic order  $b$  for the ALO and NALO matrices indicates a trend towards recombination processes in the TL peaks at lower temperatures, which gradually evolves towards a mixed recombination-trapping process for the peaks at higher temperatures.

Cerium doping produced an increase in the depth of the traps accompanied by a decrease in the TL sensitivity of the alumina matrices. In the peaks at higher temperatures it affected the deactivation mechanism favouring re-trapping in most cases.

In the future it is necessary, based on the main TL peak, to determine if the introduction of cerium produces relevant results in the use of the alumina matrix as a TL dosimeter, especially in the stabilization of the signal achieving a reduction of the thermal decay (fading) which is the major weakness reported in the literature and which is the main objective of the introduction of dopants in this type of work.

## 5. References

- [1] Daniels F, Boyd C A and Saunders D F 1953 Thermoluminescence as a Research Tool *Science* (80-). **117** 343–9
- [2] Papin E, Grosseau P, Guilhot B, Benabdesselam M, Iacconi P and Lapraz D 1996 Influence of the Calcining Conditions on the Thermoluminescence of Pure and Doped Alpha-Alumina Powders *Radiat. Prot. Dosimetry* **65** 243–6
- [3] Kortov V and Milman I 1996 Some New Data on Thermoluminescence Properties of Dosimetric Alpha-Al<sub>2</sub>O<sub>3</sub> Crystals *Radiat. Prot. Dosimetry* **65** 179–84
- [4] Duggan L, Budzanowski M, Przegietka K, Reitsema N, Wong J and Kron T 2000 The light sensitivity of thermoluminescent materials: LiF:Mg,Cu,P, LiF:Mg,Ti and Al<sub>2</sub>O<sub>3</sub>:C *Radiat. Meas.* **32** 335–42
- [5] Molnár G, Benabdesselam M, Borossay J, Lapraz D, Iacconi P and Akselrod M 2001 Influence of the irradiation temperature on TL sensitivity of Al<sub>2</sub>O<sub>3</sub>:C *Radiat. Meas.* **33** 619–23
- [6] Rocha F D and Caldas L V 1999 Characterization of Al<sub>2</sub>O<sub>3</sub> sintered pellets for dosimetric applications in radiotherapy. *J. Radiol. Prot.* **19** 51–5
- [7] Osorio A, Salcedo J and Cogollo R 2012 Pastillas sinterizadas de Al<sub>2</sub>O<sub>3</sub> como dosímetros termoluminiscentes *Ing. y Cienc.* **8** 47–64
- [8] Rocha F D G, Oliveira M L and Caldas L V E 2003 Thin sintered Al<sub>2</sub>O<sub>3</sub> pellets as thermoluminescent dosimeters for the therapeutic dose range *Appl. Radiat. Isot.* **58** 719–22
- [9] González P R, Mendoza-Anaya D, Virafuentes-Chávez H J and Azorín J 2018 Dosimetric properties of  $\alpha$ -Al<sub>2</sub>O<sub>3</sub>:Tm+PTFE phosphor *Appl. Radiat. Isot.* 0–1
- [10] Martínez-Martínez R, Rickards J, García-Hipólito M, Trejo-Luna R, Martínez-Sánchez E, Álvarez-Fregoso O, Ramos-Brito F and Falcony C 2005 RBS characterization of Al<sub>2</sub>O<sub>3</sub> films doped with Ce and Mn *Nucl. Instruments Methods Phys. Res. Sect. B Beam Interact. with Mater. Atoms* **241** 450–3
- [11] Bos A J J 2006 Theory of thermoluminescence *Radiat. Meas.* **41** S45–56
- [12] Rasheedy M S, El-Sherif M A and Hefni M A 2007 Determination of the trapping parameters of thermoluminescent glow peaks of K<sub>2</sub>YF<sub>5</sub>:Ce by three points method *Nucl. Instruments Methods Phys. Res. Sect. B Beam Interact. with Mater. Atoms* **258** 440–4
- [13] I. Lee J, L. Kim J, Y. Chang S, M. Nam Y, S. Chung K and S. Choe H 2002 Analysis of the Glow Curves Obtained from LiF:Mg,Cu,Na,Si TL Materials Using the General Order Kinetics Model *Radiat. Prot. Dosimetry* **100** 341–4
- [14] Osorio E, Gutierrez O D, Paucar C G and Hadad C Z 2009 Thermoluminescence glow curves analysis of pure and CeO<sub>2</sub>-doped Li<sub>2</sub>O-Al<sub>2</sub>O<sub>3</sub>-SiO<sub>2</sub> glass ceramics *J. Lumin.* **129** 657–60
- [15] Rojas J, Cogollo R, Gil M, Usma J, Gutiérrez O and Soto A 2019 Cerium and manganese doped alumina matrices: Preparation, characterization and kinetic analysis of their glow curves *J. Lumin.* **214** 116572
- [16] Park Y K, Tadd E H, Zubris M and Tannenbaum R 2005 Size-controlled synthesis of alumina nanoparticles from aluminum alkoxides *Mater. Res. Bull.* **40** 1506–12
- [17] Cogollo Pitalúa R, Slacedo Quintero J and Gutiérrez Flórez O 2013 Dosimetric and thermoluminescent characteristics of sintered samples *Rev. Mex. Física S* **59** 152–7